Green Chemistry

PAPER

View Article Online
View Journal | View Issue

Cite this: *Green Chem.*, 2014, **16**, 3830

Understanding the role of water during ionic liquid pretreatment of lignocellulose: co-solvent or anti-solvent?†

Jian Shi,[a,b] Kanagasabai Balamurugan,[c] Ramakrishnan Parthasarathi,[a,b] Noppadon Sathitsuksanoh,[a] Sonny Zhang,[a] Vitalie Stavila,[a,b] Venkatesan Subramanian,[c] Blake A. Simmons[a,b] and Seema Singh*[a,b]

Received 3rd March 2014,
Accepted 28th May 2014

DOI: 10.1039/c4gc00373j

www.rsc.org/greenchem

Biomass pretreatment with certain ionic liquids (IL) can be highly effective at generating a substrate that can be easily saccharified into fermentable sugars with high yields. In order to improve overall process economics, using mixtures of these ILs with water are more favored over the use of anhydrous IL; however, the solvent property of IL–water mixtures and correlations between cellulose digestibility, cellulose solvation and lignin depolymerization during IL–water pretreatment of lignocellulosic biomass are not well understood. We investigated pretreatment of switchgrass with mixtures of 1-ethyl-3-methylimidazolium acetate, [C_2mim][OAc], and water at 160 °C. Results indicate that the chemical composition and crystallinity of the pretreated biomass, and the corresponding lignin dissolution and depolymerization, were dependent on [C_2mim][OAc] concentration that correlated strongly with cellulose digestibility. In addition, the hydrogen bond basicity of the [C_2mim][OAc]–water mixtures was found to be a good indicator of cellulose dissolution, lignin depolymerization, and sugar yields. Molecular dynamics simulations provided molecular level explanations on cellulose I_β dissolution at different [C_2mim][OAc]–water loadings. The knowledge gained from this study provides a better understanding of the duality of water as a co-solvent/anti-solvent in dissolving cellulose and serves as a design basis for the targeted design of IL–water mixtures that are effective at biomass pretreatment.

1. Introduction

Liberating fermentable sugars from lignocellulosic biomass economically opens avenues for commercial scale production of biofuels and chemicals. However, the recalcitrance of biomass to enzymatic degradation poses a barrier to economical biochemical conversion technologies; thus several physical and/or chemical pretreatment processes have been implemented to disrupt the recalcitrant lignocellulosic complex and improve enzymatic digestibility.[1,2] As an emerging technology, pretreatment using certain ionic liquids (ILs), such as 1-ethyl-3-methylimidazolium acetate ([C_2mim][OAc]), shows superior performance compared to several other pretreatment technologies in terms of dramatically reducing biomass recalcitrance and enhancing enzymatic hydrolysis to fermentable sugars.[3–5] The main challenges facing IL pretreatment are the cost of ILs and system complexity associated with IL recycling, biomass–solute separation and downstream processing.[6,7]

Relying on the recent development of a thermophilic and IL-tolerant biomass-deconstructing enzyme cocktail, called JTherm,[8,9] we have developed a one-pot wash-free pretreatment and saccharification process that enables high sugar yields being achieved in the presence of 10–20% [C_2mim][OAc] IL remaining after pretreatment.[5] More recent studies have shown that lower IL concentrations (10–50% w/v) in water may also be effective in pretreating biomass, potentially reducing the amount of washing required prior to enzymatic saccharification.[10–12] Furthermore, using IL–water mixtures as pretreatment agents could reduce viscosity, eliminate gel formation during pretreatment and reduce the energy inputs and costs associated with IL recycling, facilitating scale-up and downstream processing.

To date, there have been relatively few reports on the interactions between cellulose and IL–water mixtures during cellu-

[a]*Deconstruction Division, Joint BioEnergy Institute, Emeryville, CA, USA. E-mail: seesing@sandia.gov; Fax: +1 510-486-4252; Tel: +1 925-294-4551*
[b]*Biological and Materials Science Center, Sandia National Laboratories, Livermore, CA, USA*
[c]*Chemical Laboratory, CSIR-Central Leather Research Institute, Adyar, Chennai 600 020, India*
†Electronic supplementary information (ESI) available. See DOI: 10.1039/c4gc00373j

lose regeneration after pretreatment.[13,14] Water has been considered as the driving force for separating cellulose from IL upon the addition of water as an anti-solvent,[13] and addition of up to 21 wt% water to [C_2mim]Cl–cellulose solution initiates cellulose precipitation.[15] It is also reported that the addition of water leads to the perturbation of cellulose···[OAc]$^-$ hydrogen-bonds (H-bonds) and the cellulose–cellulose interaction is enhanced at elevated temperatures.[16] Recently, Huo *et al.* examined the role of ILs, DMSO, water and mixed solvent systems on the solvation or regeneration of I_β cellulose crystals.[17] Water itself, as a pretreatment medium, can extract native hemicelluloses; at elevated temperature acetic acid is quickly liberated, further increasing hemicellulose yields, a well documented "auto-hydrolysis" phenomenon reported in the literature.[2] Hydrogen-bond basicity of the solvent system provides a direct indication of IL pretreatment efficacy, producing greater lignin/xylan removal, reduced cellulose crystallinity and improved enzymatic digestibility.[18,19]

Previous studies have demonstrated that comparable sugar yields can be achieved at reduced IL loading (<50%) in water at elevated temperatures. However, at higher temperature during IL–water pretreatment, the interplay of water as a pretreatment medium (co-solvent) and as an anti-solvent has not been comprehensively explored. In this study, we further define the role of water during ionic liquid–water pretreatment of lignocellulose as either a co-solvent or an anti-solvent. We conducted pretreatment of microcrystalline cellulose (Avicel) and switchgrass with 0, 20, 50, 80, and 100 wt% 1-ethyl-3-methylimidazolium acetate, [C_2mim][OAc], with corresponding amounts of water, at 160 °C for 3 h. The chemical composition, crystallinity and cellulose accessibility of pretreated biomass were monitored at different IL loadings and correlated to cellulose digestibility. Furthermore, Kamlet–Taft (K–T) parameters were used to predict cellulose dissolution and lignin depolymerization and correlated to sugar yields. Molecular dynamics simulations of an atomistic model of cellulose I_β dissolution at different [C_2mim][OAc] : water loadings at set temperatures were used to simulate the experimental conditions studied. This combination of experimental and computational studies provides new insight into the role of water during [C_2mim][OAc] pretreatment and provides the basis for the development of a more cost-effective route for the production of fermentable sugars from lignocellulose.

2. Results and discussion

2.1. Compositional changes

Chemical composition, solid recovery, and component removal of switchgrass before and after pretreatment with ionic liquid–water mixtures are summarized in Table 1. Pretreatment with 100% IL removed the greatest amount of biomass fractions (resulted in the lowest solid recovery of 49.3%), while reducing [C_2mim][OAc] loading led to higher solid recovery, with 20 : 80 [C_2mim][OAc]–H_2O mixture and water-only pretreatments recovering >59% of the biomass. Solids pretreated with 100% [C_2mim][OAc] had the highest glucan content while the water-only has the least. In general, all pretreated solids retained ~90% of the initial glucan content. In contrast, a large amount of xylan was removed during pretreatment; solids pretreated with 100% [C_2mim]-[OAc] contain the lowest xylan contents in accordance with the greatest xylan removal of 78.8%. Water-only pretreatment also removed a large amount of xylan, due to the "auto-hydrolysis" effects caused by the release of acetic acid during pretreatment, a phenomenon well documented in the literature.[2] Interestingly, pretreatment with 20–50% [C_2mim][OAc] was less effective at xylan removal compared with pretreatments at either higher [C_2mim][OAc] concentration or water only. We speculate that in this range the [C_2mim][OAc] provided a buffering capacity to the pH decrease associated with the release of acetic acid during pretreatment,[20] and thus reduced the extent of xylan solubilization from "auto-hydrolysis" effects, as indicated by the nearly neutral pH of the biomass liquor generated (Table 1).

ILs based on imidazolium cations, such as 1-allyl-3-methylimidazolium chloride ([C_1mim] Cl), 1-*n*-butyl-3-methylimidazolium chloride ([C_4mim]Cl), and [C_2mim][OAc], possess an excellent capacity for dissolving cellulose, partially owing to the high hydrogen-bond basicity of these ILs.[7] Furthermore, associated with cellulose dissolution, many studies have shown simultaneous removal of xylan and lignin owing to the interruption of hydrogen bonding within cellulose, hemicelluloses and lignin.[4,7] It has been demonstrated that [C_2mim]-[OAc] can effectively break down G- and S-lignin during IL pretreatment dependent on both pretreatment conditions and the type of biomass feedstocks.[21,22] Results show less lignin removal during pretreatment with a 20% [C_2mim][OAc] mixture compared with that of 100% [C_2mim][OAc]. Water-

Table 1 Chemical composition, solid recovery, and component removal of switchgrass before and after pretreatment with [C_2mim][OAc]–water mixtures[a]

	Solid recovery (%)	Glucan (%)	Xylan (%)	Klason lignin (%)
Untreated	100.0	34.6 ± 1.3	20.2 ± 0.5	19.0 ± 1.5
Water-only	59.2 ± 2.0	50.0 ± 1.1 (6.0)	10.4 ± 0.7 (69.6)	28.4 ± 0.8 (11.5)
20% IL	59.8 ± 1.1	48.5 ± 2.6 (7.9)	13.9 ± 2.3 (58.8)	21.3 ± 1.0 (33.0)
50% IL	55.4 ± 0.6	52.1 ± 0.4 (8.3)	17.9 ± 1.2 (50.9)	16.2 ± 1.0 (52.7)
80% IL	51.4 ± 1.3	55.0 ± 1.4 (10.1)	14.5 ± 0.9 (63.1)	15.7 ± 2.4 (57.5)
100% IL	49.3 ± 1.8	56.9 ± 0.7 (11.0)	8.7 ± 1.0 (78.8)	13.7 ± 0.6 (64.6)

[a] Compositions reported for untreated sample are based on the dry weight of untreated biomass; solid recoveries are based on the dry weight of untreated biomass, while the compositions for pretreated biomass are based on the dry weight of pretreated biomass; values in parentheses are percentage removal of each component (glucan, xylan or lignin) during pretreatment based on its original amount in untreated biomass.

only pretreatment removed 11.5% (the least) of lignin. Pretreatment with 50–80% [C_2mim][OAc] can remove more than 50% of the lignin from raw switchgrass, only slightly less than that of 100% [C_2mim][OAc].

2.2. Changes of cellulose crystallinity

The proportions of crystalline/amorphous cellulose and the disordered components (*i.e.* amorphous cellulose, hemicelluloses and lignin) found in pretreated switchgrass samples were determined by pXRD and expressed as the crystallinity index (CrI). Except for switchgrass pretreated with 100% [C_2mim][OAc] (showing a transition to cellulose II), all the samples pretreated with IL–water mixtures or water-only are semi-amorphous and retain primarily a cellulose I structure with different degrees of CrI (Fig. 1a). Switchgrass pretreated with 100% [C_2mim][OAc] has the lowest CrI value (16%) compared with the CrI of 0.36 of untreated switchgrass, due to the partial swelling of the cellulose matrix by [C_2mim][OAc]. Switchgrass pretreated with water-only has an increased CrI value of 0.39 compared to raw switchgrass, an effect attributed to the removal of amorphous lignin and hemicelluloses. While for solids after [C_2mim][OAc]–water pretreatment, the CrI decreases as the ratio of [C_2mim][OAc] increases in solution. The mechanism behind the CrI changes during the [C_2mim][OAc]–water pretreatment process may be determined by two competing factors: (1) swelling and dissolution of the cellulose portion (a decrease of CrI); (2) removal of the amorphous lignin and hemicelluloses (an increase of CrI). The increase in CrI values after water-only pretreatment indicates that lignin and hemicellulose removal is the dominating mechanism, an observation consistent with the compositional analysis (Table 1). Nevertheless, the decrease in CrI after pretreatment with a 50–80% [C_2mim][OAc] mixture indicates that swelling and dissolution of the cellulose (reduction in CrI) outplays the removal of amorphous components (increase in CrI). The CrI of solids resulting from pretreatment with 20% [C_2mim][OAc] remains unchanged, likely representing a balance of the two driving factors: both dissolution of the cellulose and removal of amorphous xylan and lignin (Table 1).

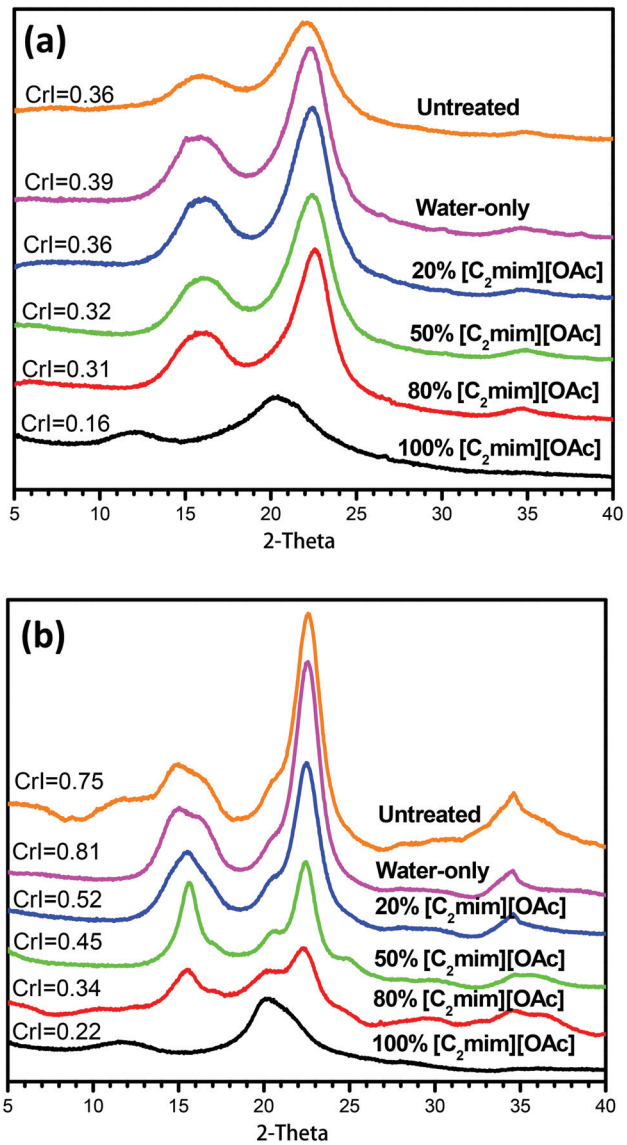

Fig. 1 Changes of cellulose crystallinity of (a) switchgrass and (b) Avicel solids pretreated with [C_2mim][OAc]–water mixtures as revealed by pXRD.

To further understand cellulose structural changes during pretreatment with [C_2mim][OAc]–water mixtures, Avicel was pretreated under the same conditions and the XRD spectra are plotted in Fig. 1b. After pretreating Avicel in 100% [C_2mim][OAc], cellulose I has been completely transformed to cellulose II as displayed in XRD patterns of the characteristic diffraction peaks at ~12.1°, 20.0°, and 21.7°.[23,24] In contrast, the crystalline structure of Avicel pretreated with water-only remained the same as untreated Avicel (*i.e.* cellulose I and amorphous). However, the crystalline structures of Avicel pretreated with IL–water mixtures showed partial features of both cellulose I/amorphous and cellulose II. It is also seen that a clear trend of decrease in CrI follows the ratio of IL in the water solution. These results indicate that although [C_2mim][OAc] is capable of dissolving or swelling cellulose, the presence of water, as an anti-solvent, conversely, decreases the effectiveness of cellulose dissolution and retards the transformation of cellulose I to amorphous/cellulose II.

2.3. Solvent properties of [C_2mim][OAc]–water mixtures

Certain solvent properties, such as solvatochromic properties, describe solute–substrate hydrogen bonding interactions. The Kamlet–Taft system bins these properties into three separate terms: polarizability (π^*), hydrogen bond donator capacity (α) and hydrogen bond acceptor capacity (β).[25] Although the Kamlet–Taft procedure was initially designed for measuring solvent properties of a single solvent, it has been applied for describing the average or bulk solvent properties of binary and ternary solvent mixtures.[11,26] The solvent properties of the [C_2mim][OAc]–water mixtures studied are summarized in Table 2. We found that π^* decreased as water content increased. A similar behavior was observed for β; these values

Table 2 Solvent properties of [C_2mim][OAc]–water mixtures at 160 °C[a]

	pH		π: Solvent polarizability	α: Hydrogen bond donor capacity	β: Hydrogen bond acceptor capacity
	A	B			
Water-only	6.86	4.09	0.67	1.46	0.97
20% IL	6.89	5.50	0.69	—	1.01
50% IL	8.15	6.22	0.73	0.88	1.04
80% IL	9.22	6.73	0.78	0.74	1.15
100% IL	11.55	7.13	0.84	0.51	1.23

[a] π, α, and β parameters were extrapolated from actual measurement at 30, 60, 90, 110 °C or up to 80 °C for water; the pH values were extrapolated from actual measurements of the 1 : 1 dilution of (A) the IL–water mixtures and (B) the hydrolysate after pretreatment of switchgrass; (α) value of 20% [C_2mim][OAc] in water could not be determined since no peak was observed with Reichardt's dye.

have been considered to be a good predictor of IL pretreatment efficacy with higher β (>1.0) values correlated to: (1) greater lignin/xylan removal; (2) reduced cellulose crystallinity; and (3) improved enzymatic digestibility. Doherty *et al.*[27] have proposed that ILs with higher β values form strong attractions between anions and the hydroxyl protons of cellulose, leading to disruption of the crystal lattice. In addition, Sun and co-workers (2014) established links between computationally predicted interaction energies and the experimentally determined Kamlet–Taft parameters and showed a positive correlation between glucose yield and β values.[19] Results from this study suggest that the same rules may apply to pretreatment with IL–water mixtures, with positive linear correlations observed between β values and lignin removal and initial glucose yield (Fig. 4). As reported previously, the β value is primarily determined by the anion[28–30] and ILs with higher β values,[31] and more recently ILs with larger differences between β and α, net basicity ($\beta - \alpha$),[32,33] tend to dissolve cellulose more efficiently. Our results suggest that although the β values decreased for IL–water mixtures as a function of water content, it can be used to predict the pretreatment efficiency and define an effective range of concentrations to conduct pretreatment.

2.4. Lignin dissolution and depolymerization

The differences seen in lignin removal and CrI patterns in the previous sections merited further investigation into the impact of IL–water mixtures on lignin dissolution and depolymerization. Lignin dissolution caused by the cleavage of specific inter-unit lignin linkages and lignin carbohydrate cross-links has been widely investigated on water-only pretreatment.[34–36] The mechanism of lignin depolymerization during [C_2mim][OAc] pretreatment was recently examined[22,37,38] and preferential lignin dissolution was often observed due to the chemical nature of lignin according to building blocks and the inter-unit linkages.[38] In order to monitor the lignin molecular weight distribution as a function of pretreatment using different [C_2mim][OAc]–water contents, size exclusion chromatography (SEC) was performed on lignin solubilized in aqueous [C_2mim][OAc] and remaining in pretreated solids (Fig. S1†). Excluded ($A_{Excluded}$) and retained ($A_{Retained}$) regions are defined using the retention time of 13.4 min (u = ~46k by polystyrene calibration). Decreases in the ratios of the relative area ($A_{Excluded/Retained}$ ($A_{E/R}$)) of the mass peak of larger molecular mass lignin products (t < 13.4 min) to smaller molecular mass lignin products (t > 13.4 min) for the lignin fraction compared to that of enzymatic mild acidolysis lignin (EMAL), are a broad gauge for depolymerization. The $A_{E/R}$ were reported in Table 3 as an indicator of the relative molecule weight distribution of solubilized lignin in aqueous [C_2mim][OAc] or lignin that remained in the solid stream. EMAL of untreated switchgrass samples showed a strong signal in the excluded region (t < 13.4 min) with an $A_{E/R}$ of 2.43, suggesting that EMAL of untreated switchgrass consisted mainly of large molecular weight materials. As for the lignins solubilized in IL–water during pretreatment, a distinct signal in the retained region (t > 13.4 min) was observed with reduced $A_{E/R}$ in a range of 0.46 to 0.92 for different [C_2mim][OAc]–water mixtures compared to that of EMAL. The lower $A_{E/R}$ in solubilized lignin indicates that lignin was solubilized and depolymerized in the liquid stream during pretreatment.[5,39] Interestingly, the $A_{E/R}$ for the lignin solubilized in 100% [C_2mim][OAc] or water-only was lower than that solubilized in 20–80% [C_2mim][OAc], indicating different possible lignin dissolution or depolymerization mechanisms.

The lignin residues in all pretreated solids showed higher $A_{E/R}$ (greater than 1) compared with the soluble lignin (less than 1). Furthermore, compared to EMAL of untreated switchgrass, residual lignin in pretreated solids exhibited lower $A_{E/R}$, indicating that the pretreated switchgrass contained smaller molecular weight material than the EMAL, supporting small

Table 3 Elution time and relative molecular mass of lignin solubilized during pretreatment using [C_2mim][OAc]–water mixtures[a]

	Lignin solubilized in pretreatment hydrolysate			Lignin retained in untreated/pretreated solids		
Regions with elution time (min)	Excluded (%) t < 13.4 (u > 46k)	Retained (%) t < 13.4 (u > 46k)	$A_{E/R}$	Excluded (%) t < 13.4 (u > 46k)	Retained (%) t < 13.4 (u > 46k)	$A_{E/R}$
EMAL switchgrass	N/A	N/A	N/A	70.9	29.1	2.43
Water-only	34.2	65.8	0.52	63.6	36.4	1.75
20% IL	41.3	58.7	0.70	66.5	33.5	1.99
50% IL	48.0	52.0	0.92	59.8	40.2	1.49
80% IL	41.0	59.0	0.69	58.5	41.5	1.41
100% IL	31.3	68.7	0.46	45.3	54.7	0.83

[a] $A_{E/R}$ stands for the ratio of peak areas in the excluded and retained regions; N/A stands for not available.

molecular weight lignin materials observed in the liquid streams. It is possible that either branches or end-units have been removed from the recalcitrant lignin "backbone", reducing its molecular mass but not allowing it to fully solubilize, a phenomenon reported previously.[39] Moreover, $A_{E/R}$ of residual solids after 100% IL pretreatment was much smaller than that of residual solids pretreated by [C_2mim][OAc]–water mixtures, suggesting that adding water negatively influences the effectiveness of delignification and lignin depolymerization.[19]

2.5. Cellulose accessibility and substrate characteristics

We used solid-state ^{13}C CP/MAS NMR in conjugation with FTIR spectra to evaluate the cellulose accessibility and substrate characteristics of [C_2mim][OAc]–water pretreated switchgrass. The NMR spectrum reveals ^{13}C chemical shifts of cellulose carbons (Fig. 2a), including C1 (105 ppm), C4 (79–92 ppm), C2/C3/C5 (70–80 ppm), and C6 (60–69 ppm) with the C4 and C6 resonance regions commonly used for determining cellulose crystallinity.[40–42] The NMR spectrum of raw switchgrass showed strong signals at 89 and 65 ppm and broad signals at 83 and 63 ppm, indicating that raw switchgrass contains both crystalline and amorphous fractions, which is in agreement with that previously reported.[43] It is evident that the crystalline peaks decreased and the amorphous peaks increased in C4 and C6 regions for switchgrass samples treated with 100% [C_2mim][OAc], indicating that highly ordered hydrogen-bonding networks in switchgrass were disrupted by [C_2mim][OAc]. We also observed a gradual transition of crystalline and amorphous peaks of switchgrass pretreated with 0–100% [C_2mim][OAc], suggesting the gradual decreases of solvation power of [C_2mim][OAc]–water mixtures from high to low [C_2mim][OAc] concentrations. A comparison of FTIR spectra of [C_2mim][OAc]–water pretreated switchgrass shows differences in band intensities at 900 cm^{-1} (C–H deformation in cellulose), 1056 cm^{-1} (C–O stretching in cellulose and hemicelluloses), 1098 cm^{-1} (C–O vibration of crystalline cellulose), 1329 cm^{-1} (syringyl and guaiacyl condensed lignin), and 1510 cm^{-1} (aromatic skeletal of lignin).[4] Fig. 2b shows that the band intensities at 1056 and 1098 cm^{-1} decrease from raw switchgrass to 100% [C_2mim][OAc] pretreated switchgrass, implying that highly ordered hydrogen bonds in raw switchgrass were disrupted through cellulose dissolution and regeneration.[43] The 50–80% [C_2mim][OAc]–water pretreated sample showed more significant decreases in the band intensities at 1098 and 1056 cm^{-1} than raw SG, suggesting that highly ordered hydrogen bonds in crystalline cellulose of switchgrass were disrupted after the pretreatment.

2.6. Enzymatic digestibility

As expected, pretreatment with 100% IL led to very high cellulose digestibility when pretreated solids were subjected to enzymatic hydrolysis at both low and high enzyme loadings (Fig. 3). It is also noticed that the glucose yield curve reach a plateau after 24 h, a result matching previous reports on the nearly complete saccharification within 24 h.[44] The fast hydrolysis kinetics is due to the regeneration of easily digestible type

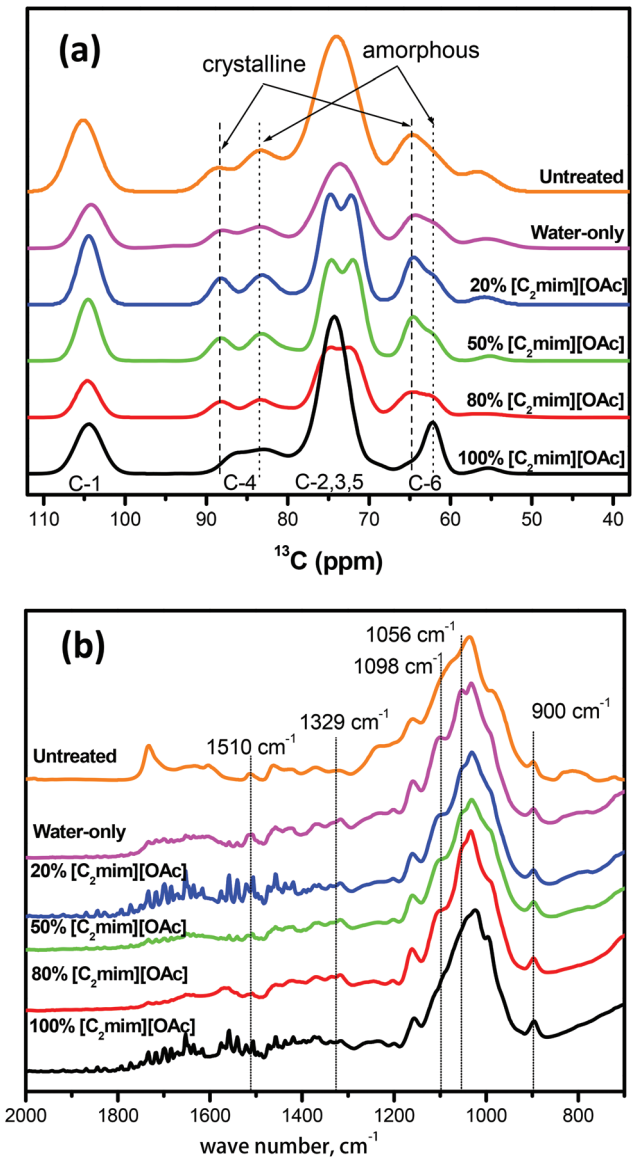

Fig. 2 (a) Solid-state ^{13}C CP/MAS NMR and (b) FTIR spectra of untreated switchgrass and switchgrass pretreated with [C_2mim][OAc]–water mixtures.

II/amorphous cellulose when cellulose is treated with ionic liquid.[4,24] Interestingly, 85–90% glucose yields were achieved for pretreatment with 50–80% [C_2mim][OAc] at 20 mg enzyme per g biomass. However, much lower glucose yields were seen for pretreatment with water-only or 20% [C_2mim][OAc]. Notably, fast sugar releases in the first 24 h were also observed for solid pretreated with 50–80% [C_2mim][OAc] as compared with that of water-only pretreatment, indicating that these solids were readily saccharified. Results from the study were in general agreement with previous reports using [C_2mim][OAc] and water as pretreatment media.[10,45] However, higher than 85% glucose yield, within 24 h, can only be achieved using 60–90% [C_4mim][$MeSO_4$] or [C_4mim][HSO_4] in water,[11] indicating that the pretreatment efficiency is also dependent on the selection of ILs as well as the presence of water.

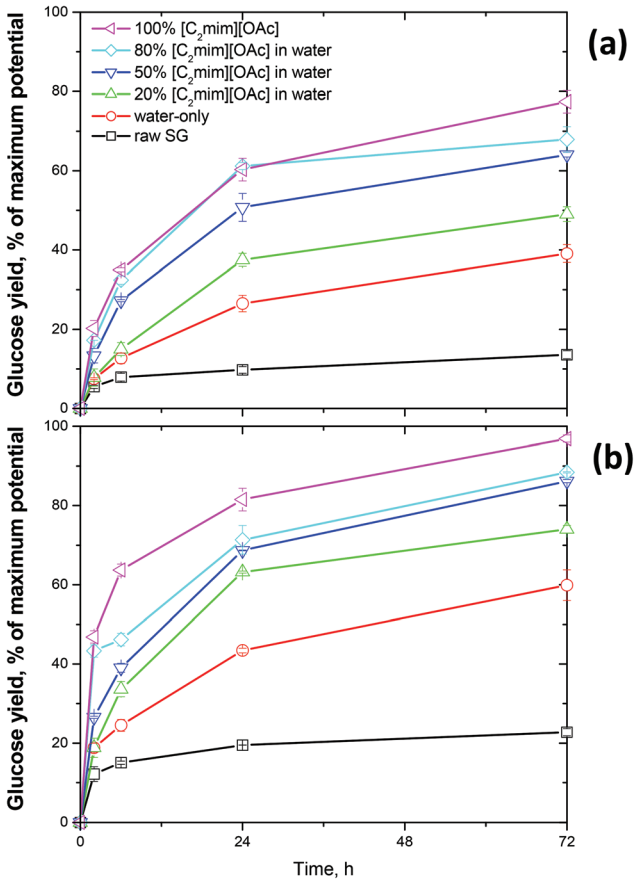

Fig. 3 Glucose yield from enzymatic hydrolysis of untreated switchgrass and switchgrass solids pretreated with [C_2mim][OAc]–water mixtures at (a) 5 mg and (b) 20 mg enzyme protein per g initial biomass.

Associated with the compositional changes, it is inferred that the initial glucose yields (average % per hour glucose release in the first two hours) were positively correlated to lignin removal (Fig. 4a). However, it seems that only at >50% lignin removal the initial glucose yields can be significantly increased, an observation that matches the high overall glucose yield and fast saccharification kinetics seen for pretreatment with 100% [C_2mim][OAc] or 50–80% [C_2mim][OAc] mixtures. Furthermore, there is a positive linear correlation between the initial glucose yields and β values, indicating that β values could be used to predict the pretreatment efficiency for the [C_2mim][OAc]–water mixture (Fig. 4b). No strong correlations were seen between xylan removal/CrI and the initial glucose yields (Fig. 4c and d), probably due to the very different mechanisms behind water-only pretreatment and pretreatment with 100% [C_2mim][OAc] or [C_2mim][OAc]–water mixtures. Although cellulose with a high amorphous content is usually more easily digested by enzymes, it is clear that CrI is not a reliable sole indicator of digestibility, especially for lignocellulosic biomass, based on studies published in the literature.[42,46] Cellulose digestibility can be affected by crystallinity, but is also affected by several other parameters, such as

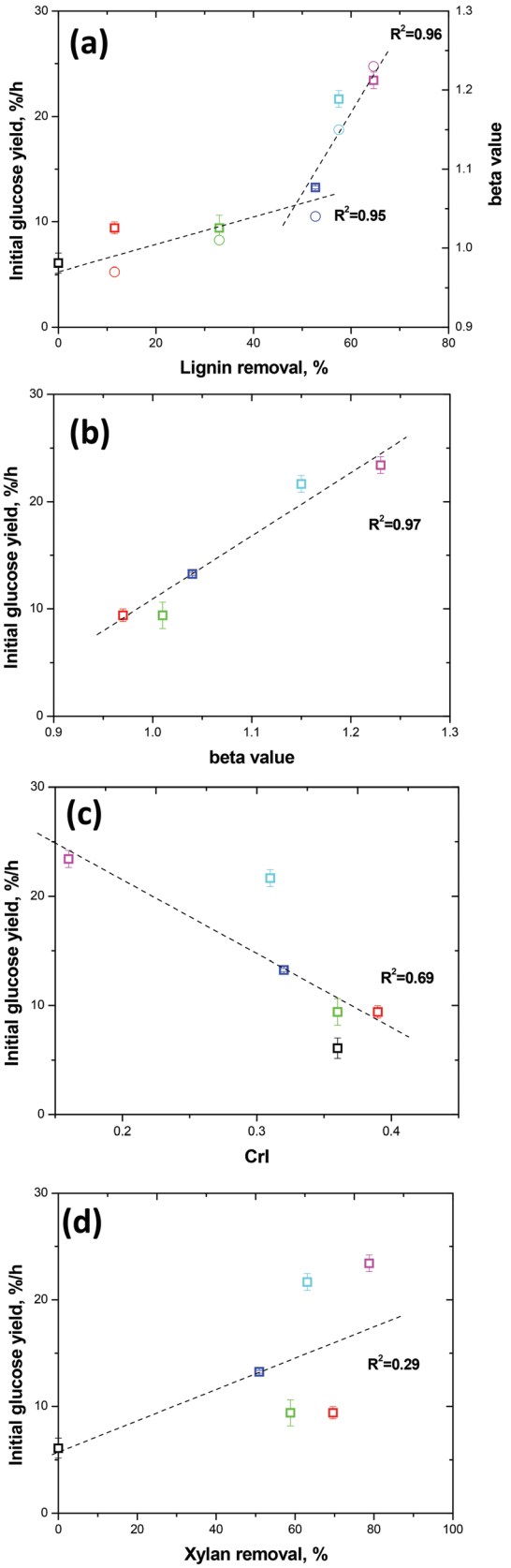

Fig. 4 Correlation between the initial enzymatic cellulose digestibility with (a) lignin removal, (b) β value of the K–T parameters, (c) CrI, and (d) xylan removal.

lignin/hemicellulose contents and distribution, porosity, and particle size.[2,46]

2.7. Molecular dynamics simulation of cellulose dissolution in IL–water mixtures

Experimental and theoretical studies have been carried out to understand the interactions between cellulose and ILs.[13,47] Cellulose chains form stronger interaction with the IL than with water. For instance, the acetate anion forms strong hydrogen bonding interactions with the hydroxyl groups of cellulose and some of the cations were found to be in close contact with the cellulose through hydrophobic interactions.[13] In this work, classical MD simulation has been performed to gain an atomistic level understanding of the dissolution of cellulose model matrices composed of cellulose I_β in different [C_2mim][OAc] and water concentrations (Fig. S2†). The results of inter-chain and total H-bonds in the cellulose matrix during the course of simulation (Fig. 5) show that the reduction in the number of H-bonds is directly proportional to the concentration of [C_2mim][OAc] which is in accordance with the earlier reports.[13] It is interesting to note that the trend in the decrease of total H-bonds is similar to the inter-chain H-bonds. However, a close scrutiny of the plot of inter-chain H-bonds with time shows that there are no appreciable changes in the number of H-bonds observed in the case of simulation in 100%, 80%, and 50% [C_2mim][OAc]. The above results reveal that the dissolution of the cellulose bundle into individual cellulose chains in both 50% and 80% [C_2mim][OAc] in water is comparable to that of 100% [C_2mim][OAc]. Our results are in agreement with previous simulations on cellulose–IL dissolution, in which ILs influenced intermolecular and intramolecular interactions of cellulose,[13] and also complementary to the experimental trend reported here for different concentrations of the [C_2mim][OAc]–water mixture. It is well known that the degree of polymerization (DP) influences the solvation. Cellulose with DP < 6 are quite soluble in water and the water solubility of cellulose decreases as the chain-length increases.[43] These results indicate that the dissolution of cellulose with DP = 6 occurs in accordance with concomitant solvation properties. However, the results may quantitatively vary with higher DP.

Another important focus of our study is to elucidate the role of water in cellulose dissolution of [C_2mim][OAc]. We carried out an additional analysis (Fig. 6) of dissecting water interactions with anions, cations, and cellulose from different [C_2mim][OAc]–water mixtures. The water interaction with ions is typically one of the rate-limiting steps preceding regeneration of cellulose.[32,48] This additional analysis has ramifications on the role of water interaction and its relationship to the overall solvation efficiency in various [C_2mim][OAc]–water concentrations. We found that interaction energies of water with cellulose chains were increased gradually with the increase in the concentration of water, but interestingly, it enhanced interactions with [OAc] and [C_2mim] ions at 50% of water concentration. Results indicate that as IL–water mixtures, less than 50% of water with [C_2mim][OAc] supports dissolution of the cellulose model system simulated in this work, whereas water concentrations higher than 50% enhance interactions of water molecules with ions but weaken cellulose–[C_2mim][OAc] interactions. As illustrated in Fig. 6 on hydrogen bonding interactions with anion/cellulose, at lower concentration, water acts as a (co-)solvent which helps to facilitate the disintegration of strong ionic anion–cation association of [C_2mim][OAc]. Moreover, taking into the consideration that

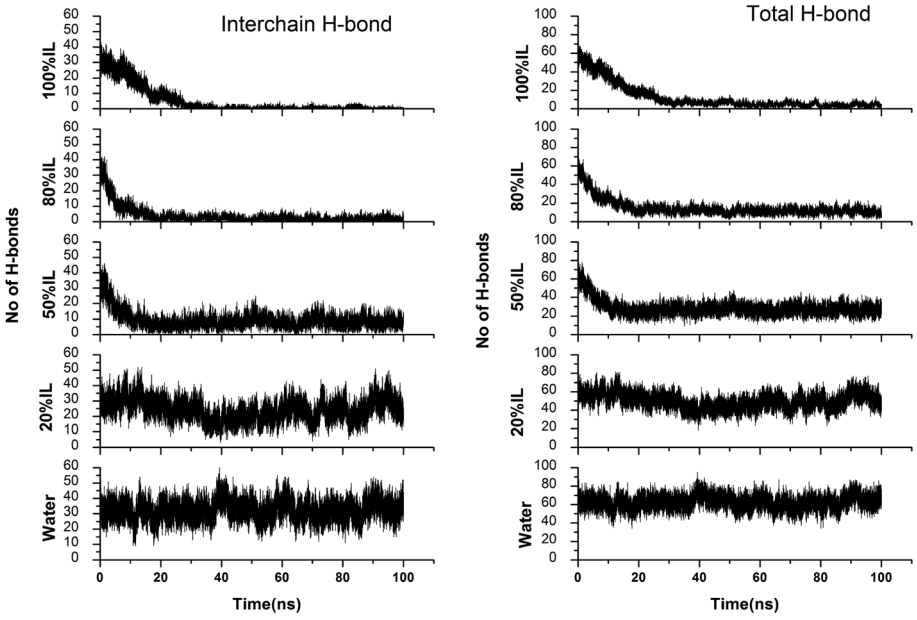

Fig. 5 Effect of [C_2mim][OAc]–water mixtures on disrupting the inter-chain H-bonds and total H-bonds between cellulose at 160 °C based on model simulation with cellulose I_β consisting of 9 chains with each chain having a polymerization of 6 glucose units.

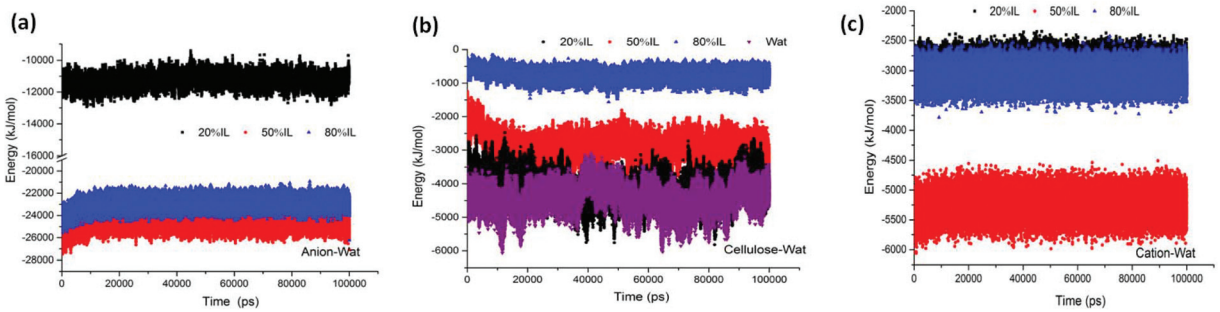

Fig. 6 Analysis for dissecting the role of water interactions with (a) anions, (b) cellulose and (c) cations in different [C_2mim][OAc]–water mixtures.

water molecules strongly solvate the ions, it is conceivable that above 50% concentration, water reduces the hydrogen bonding interactions between [C_2mim][OAc] and cellulose. Our simulation predicts that a reduction in the effective IL dissolution of cellulose is coupled with increasing water molecule interactions with the anions, cations and cellulose (a schematic of the proposed IL–water dissolution mechanism of cellulose; Fig. S2†). The present results thus suggest a synergistic solution on the limit of minimum/maximum [C_2mim][OAc]: water loading to improve the cellulose dissolving capability of ILs.

3. Conclusions

Our results show that pretreatment with 50–80% [C_2mim][OAc] aqueous mixtures at 160 °C can match the performance of 100% [C_2mim][OAc] in terms of glucose yield. The ratio of [C_2mim][OAc] in water plays a critical role in cellulose solubilization, lignin and xylan removal, crystallinity, and cellulose accessibility, and in combination greatly affects the enzymatic digestibility. The hydrogen bond basicity (β value), representing the ability to disrupt the inter- and intra-molecular hydrogen bonding in cellulose, hemicellulose and lignin, correlates well with cellulose crystallinity, lignin removal and serves as a good indicator of pretreatment efficacy for [C_2mim][OAc]–water mixtures. Molecular dynamics simulations provide molecular level explanations on cellulose I_β dissolution at different [C_2mim][OAc]–water loadings at set temperatures which shows that IL–water mixtures can be efficiently used for the solubilization of cellulose microfibrils into individual chains. Our findings provide new insights into the interplay of water as a co- and anti-solvent, respectively, below and above 50% [C_2mim][OAc] concentration in the chosen model systems for the dissolution of cellulose. On considering the importance of dissolution of the cellulose bundle into individual chains for the efficient enzymatic hydrolysis of polysaccharides and taking into account the cost of using IL, it is feasible to employ [C_2mim][OAc] in the range of 50–80% in water to achieve an efficient dissolution of cellulose in an economically viable process.

4. Experimental

4.1. Materials

Switchgrass (*Panicum virgatum*) was provided by Dr Daniel Putnam, University of California at Davis. Switchgrass was ground by a Wiley Mill through a 2 mm screen and separated by a vibratory sieve system (Endecotts, Ponte Vedra, FL). The switchgrass fractions falling between 20 and 80 mesh were collected for use in this study. The moisture content of switchgrass was measured as 6.7%. Avicel PH101 (Lot no. 1344705, Sigma-Aldrich, St. Louis, MO) is a microcrystalline cellulose (MCC) containing more than 97% cellulose and less than 0.16% water soluble materials. 1-Ethyl-3-methylimidazolium acetate, abbreviated hereafter as [C_2mim][OAc], was purchased from BASF (Basionics™ BC-01, BASF, Florham Park , NJ) and used as the IL for all pretreatments. The water content of [C_2mim][OAc] was measured as 0.7% using a titrator (870 KF Titrino plus, Metrohm USA Inc., Riverview, FL) and was counted to the final water concentration in [C_2mim][OAc]–water mixtures. Commercial enzyme products, cellulase (Cellic® CTec2, Batch#VCN10007) and hemicellulase (Cellic® HTec2, Batch#VHN00002) were gifts from Novozymes, North America (Franklinton, NC).

4.2. Pretreatment with IL–water mixtures

IL–water mixtures were prepared by mixing [C_2mim][OAc] with DI water at different ratios to give five levels (0, 20, 50, 80, 100 wt%, equivalent to 0, 0.024, 0.096, 0.297, and 1 mole fraction, respectively) of IL in water. Two grams of switchgrass (dry basis) were mixed with 18 grams of [C_2mim][OAc]–water solution to give a 10 wt% biomass loading in tubular reactors made of 1 inch diameter × 4 inch length stainless steel (SS316) tubes. The tubes were then sealed with stainless steel caps. All pretreatments were run in triplicate in tubular reactors that were heated to reaction temperature using a fluidized sand bath with temperature set circa 2 °C higher than the pretreatment temperature to hold the reaction at the target temperature as measured using a thermocouple. The heat-up time was ~8–10 min and is not included in the stated reaction times. After pretreatment, the reactors were quenched by quickly transferring them to a room temperature water bath until the

temperature dropped to 30 °C (the cooling time was around 1–2 min and was not included in the stated reaction time).

To separate solids from liquid after pretreatment, the pretreated biomass was transferred to a 50 ml centrifuge tube and by adding 20 ml hot water to the samples as an anti-solvent for cellulose regeneration and for recovering any solubilized biomass. The mixture of [C_2mim][OAc], water, and pretreated biomass was centrifuged to separate the solids and liquid phases. The liquid phase, namely pretreatment liquid, was collected and store at 4 °C for sugar analysis. The solid fraction was washed four times with 45 ml of hot water to remove any excess [C_2mim][OAc]. An aliquot of recovered solid was lyophilized in a FreeZone Freeze Dry System (Labconco, Kansas City, MO) and used for composition and X-ray diffraction (XRD) analysis.

4.3. X-ray powder diffraction measurements

XRD data were collected with a PANalytical Empyrean X-ray diffractometer equipped with a PIXcel^{3D} detector and operated at 45 kV and 40 kA using Cu Kα radiation (λ = 1.5418 Å). The patterns were collected in the 2θ range of 5 to 55°, the step size was 0.026°, with an exposure time of 600 seconds. A reflection–transmission spinner was used as a sample holder and the spinning rate was set at 8 rpm throughout the experiment. The crystallinity index (CrI) was determined from the crystalline and amorphous peak areas by a curve fitting procedure of the measured diffraction patterns using the software package HighScore Plus®. Since the XRD peak height method is unsuitable for determining the CrI values of cellulose II or cellulose I/II mixtures, we used the crystalline area method previously described elsewhere, using crystalline cellulose I (Avicel), cellulose II (prepared previously in our laboratory[24]) and amorphous (lignin) as representative samples.[42] The CrI values reported in this study reflect the ratio of the areas of the crystalline fractions (with the amorphous component subtracted) to the total area of the measured XRD patterns.

4.4. Solid-state ^{13}C CP/MAS NMR and FTIR

The cross-polarization magic-angle spinning (CP/MAS) ^{13}C-NMR spectra of all samples were obtained on a Bruker II Avance-300 spectrometer operating at the resonance frequencies of 300.12 MHz for 1H, and 75.47 MHz for 13C, using a Bruker 4.0 mm MAS NMR probe spinning at 6 kHz. Cross-polarization for 1 ms mixing time was achieved at 50 kHz rf-field at the 1H channel and linearly ramping the 13C rf-field over a 25% range centered at 38 kHz. Total accumulation time was 8 min (2048 transient signals) by using 63 kHz of the two-pulse phase modulated proton decoupling technique.[49] All spectra were collected at room temperature with polyethylene as an internal standard. According to the NMR amorphous subtraction method, the amorphous contribution was separated from the original spectrum prior to deconvolution of signals in the C4 resonance region, where xylan was an amorphous standard.[41] Attenuated total reflection-Fourier transform infrared spectroscopy (ATR-FTIR) of switchgrass samples was conducted using a Bruker Optics Vertex system with built-in diamond–germanium ATR single reflection crystal by following a procedure described elsewhere.[4]

4.5. Enzymatic hydrolysis

Enzymatic saccharification of pretreated and untreated biomass samples was run in duplicates by following NREL LAP 9 "Enzymatic Saccharification of Lignocellulosic Biomass" under NREL standard conditions (50 °C, 0.05 M citrate buffer, pH 4.8).[50] Citrate buffer (final molarity 50 mM), sodium azide (antimicrobial, final concentration of 0.01 g l^{-1}), enzymes, and DI water were mixed with pretreated solids to achieve a final solids loading of around 5% (equivalent to 2.5% (w/w) glucan concentration). CTec2 and HTec2 were used at enzyme loadings of 5 and 20 mg CTec2 protein per g starting biomass supplemented with HTec2 at loadings of 0.07 and 0.26 mg enzyme protein per g glucan, respectively. The supernatant collected during 72 h of hydrolysis was analyzed with HPLC for the monosaccharide as described in the analytical method section below. Enzymatic digestibility was defined as the glucose yield based on the maximum potential glucose from glucan in biomass.

4.6. Analytical methods

The saccharification hydrolysate was separated by centrifugation at 14 000g for 10 min followed by syringe filtration. The amount of cellobiose, glucose, xylose, and arabinose released in the hydrolysate was measured using an Agilent 1100 series HPLC equipped with a Biorad Aminex HPX-87H ion exchange column and a refractive index detector, using 4 mM H_2SO_4 as the mobile phase at a flow rate of 0.6 ml min^{-1} and a column temperature of 60 °C.[51]

4.7. Characterization of lignin in liquid and residual solids

To understand the changes in lignin molecular weight distribution during pretreatment, size exclusion chromatography (SEC) was performed on the lignin in both liquid stream and residual solids after IL pretreatment. An Agilent 1200 series binary LC system (G1312B) equipped with a DA (G1315D) detector was used. Separation was achieved with a Mixed-D column (5 μm particle size, 300 mm × 7.5 mm i.d., linear molecular weight range of 200 to 400 000 u, Polymer Laboratories, Amherst, MA) at 80 °C using a mobile phase of NMP at a flow rate of 0.5 ml min^{-1}. The elution profile of materials eluting from the column was monitored by UV absorbance at 290 nm (UV-A_{290}). Intensities were area normalized and the molecular weight was determined after calibration of the system with polystyrene standards.[39] The enzymatic mild acidolysis lignin (EMAL) process was used to extract lignin from switchgrass and it was used as a control.[52]

4.8. Kamlet–Taft (K–T) parameters measurement

Parameters derived from the Kamlet–Taft procedure, namely K–T parameters, provide a quantitative measurement of solvent polarizability (π*), hydrogen bond donator capacity (α)

and hydrogen bond acceptor capacity (β). K–T parameters were determined spectrophotometrically using a series of dyes according to previous reports.[18,27] The three dyes: 4NA, DENA, and RD solutions, were prepared in ethanol to a concentration of 1 mg ml^{-1}. 2 μl of 4NA, 2 μl of DENA and 20 μl of RD were pipetted into three separate vials and the ethanol was evaporated under a stream of dry nitrogen. Dye concentrations of 12 mM, 8 mM, and 28 mM, respectively, were obtained by adding 1.25 ml of the [C_2mim][OAc]–water mixtures to each vial and mixing on a shaker at 300 RPM for 30 min. The absorbance spectra at 30–110 °C of each IL/dye solution were measured between 350 and 700 nm using a spectrophotometer equipped with a temperature controller (TMSPC-8, Shimadzu Corporation). K–T parameters for higher temperatures were estimated using linear regression of the parameter values between 30 and 110 °C.[22]

4.9. Computational methods

Molecular dynamics simulation of the cellulose I_β with 9 chains was taken as a model system in which each chain has a degree of polymerization of 6 (6 glucose units). The cellulose was immersed in a box of size 34 × 48 × 52 Å and solvated with [C_2mim][OAc]–water solvent systems of various concentrations (water, 20% IL, 50% IL, 80% IL and 100% IL). MD simulations were carried out using Gromacs 4.6 suite of package.[53,54] For the simulation, GLYCAM forcefield was used for the cellulose.[55] The GAFF parameters[56] with charges from Liu *et al.*[13] were used for IL and the water molecules were treated using TIP3P parameters.[57] A 2 fs time step was used to integrate the equation of motion. Electrostatic interaction was calculated using Particle Mesh Ewald sums[58] with a nonbonded cut-off of 10 Å. Bonds between hydrogen and heavy atoms were constrained at their equilibrium length using the LINCS algorithm.[59] Equilibration was performed for 250 ps in NVT ensemble and the temperature was increased from 300 to 433 K. Further, 500 ps of equilibration was carried out in NPT ensemble. Subsequently, 100 ns of production run was carried out in NPT ensemble for all the systems. The pressure was retained at 1 atm and the temperature was retained at 433 K using a Parrinello–Rahman barostat and a V-rescale thermostat, respectively.[60] The trajectories were saved every 1 ps for further analysis. The results were visualized using pymol.[56]

Acknowledgements

This work conducted by the Joint BioEnergy Institute was supported by the Office of Science, Office of Biological and Environmental Research, of the U.S. Department of Energy under contract no. DE-AC02-05CH11231. This research used resources of the National Energy Research Scientific Computing Center (NERSC). We acknowledge Dr Ping Yu at UC Davis for conducting solid state NMR measurements and Taylor Cu for the assistance in lab work.

References

1 M. E. Himmel, S. Y. Ding, D. K. Johnson, W. S. Adney, M. R. Nimlos, J. W. Brady and T. D. Foust, *Science*, 2007, **315**, 804–807.
2 J. Shi, M. A. Ebrik, B. Yang, R. J. Garlock, V. Balan, B. E. Dale, V. R. Pallapolu, Y. Y. Lee, Y. Kim, N. S. Mosier, M. R. Ladisch, M. T. Holtzapple, M. Falls, R. Sierra-Ramirez, B. S. Donohoe, T. B. Vinzant, R. T. Elander, B. Hames, S. Thomas, R. E. Warner and C. E. Wyman, *Bioresour. Technol.*, 2011, **102**, 11080–11088.
3 S. Singh, B. A. Simmons and K. P. Vogel, *Biotechnol. Bioeng.*, 2009, **104**, 68–75.
4 C. L. Li, B. Knierim, C. Manisseri, R. Arora, H. V. Scheller, M. Auer, K. P. Vogel, B. A. Simmons and S. Singh, *Bioresour. Technol.*, 2010, **101**, 4900–4906.
5 J. Shi, J. M. Gladden, N. Sathitsuksanoh, P. Kambam, L. Sandoval, D. Mitra, S. Zhang, A. George, S. W. Singer, B. A. Simmons and S. Singh, *Green Chem.*, 2013, **15**, 2579–2589.
6 D. Klein-Marcuschamer, B. A. Simmons and H. W. Blanch, *Biofuels Bioprod. Bioref.*, 2011, **5**, 562–569.
7 S. Singh and B. A. Simmons, in *Aqueous Pretreatment of Plant Biomass for Biological and Chemical Conversion to Fuels and Chemicals*, ed. C. E. Wyman, 2013.
8 J. I. Park, E. J. Steen, H. Burd, S. S. Evans, A. M. Redding-Johnson, T. Batth, P. I. Benke, P. D'haeseleer, N. Sun, K. L. Sale, J. D. Keasling, T. S. Lee, C. J. Petzold, A. Mukhopadhyay, S. W. Singer, B. A. Simmons and J. M. Gladden, *PLoS One*, 2012, **7**, e37010.
9 J. M. Gladden, M. Allgaier, C. S. Miller, T. C. Hazen, J. S. VanderGheynst, P. Hugenholtz, B. A. Simmons and S. W. Singer, *Appl. Environ. Microbiol.*, 2011, **77**, 5804–5812.
10 D. B. Fu and G. Mazza, *Bioresour. Technol.*, 2011, **102**, 8003–8010.
11 A. Brandt, M. J. Ray, T. Q. To, D. J. Leak, R. J. Murphy and T. Welton, *Green Chem.*, 2011, **13**, 2489–2499.
12 X. D. Hou, N. Li and M. H. Zong, *Bioresour. Technol.*, 2013, **136**, 469–474.
13 H. Liu, K. L. Sale, B. M. Holmes, B. A. Simmons and S. Singh, *J. Phys. Chem. B*, 2010, **114**, 4293–4301.
14 M. Abe, Y. Fukaya and H. Ohno, *Chem. Commun.*, 2012, **48**, 1808–1810.
15 M. Mazza, D. A. Catana, C. Vaca-Garcia and C. Cecutti, *Cellulose*, 2009, **16**, 207–215.
16 K. M. Gupta, Z. Q. Hu and J. W. Jiang, *RSC Adv.*, 2013, **3**, 4425–4433.
17 F. Huo, Z. P. Liu and W. C. Wang, *J. Phys. Chem. B*, 2013, **117**, 11780–11792.
18 T. V. Doherty, M. Mora-Pale, S. E. Foley, R. J. Linhardt and J. S. Dordick, *Green Chem.*, 2010, **12**, 1967–1975.
19 N. Sun, R. Parthasarathi, A. M. Socha, J. Shi, S. Zhang, V. Stavila, K. L. Sale, B. A. Simmons and S. Singh, *Green Chem.*, 2014, **16**, 2546–2557.
20 P. Kilpelainen, V. Kitunen, A. Pranovich, H. Ilvesniemi and S. Willfor, *Bioresources*, 2013, **8**, 5202–5218.

21 G. Papa, P. Varanasi, L. Sun, G. Cheng, V. Stavila, B. Holmes, B. A. Simmons, F. Adani and S. Singh, *Bioresour. Technol.*, 2012, **117**, 352–359.
22 P. Varanasi, P. Singh, R. Arora, P. D. Adams, M. Auer, B. A. Simmons and S. Singh, *Bioresour. Technol.*, 2012, **126**, 156–161.
23 P. Mansikkamäki, M. Lahtinen and K. Rissanen, *Cellulose*, 2005, **12**, 233–242.
24 G. Cheng, P. Varanasi, C. L. Li, H. B. Liu, Y. B. Menichenko, B. A. Simmons, M. S. Kent and S. Singh, *Biomacromolecules*, 2011, **12**, 933–941.
25 M. J. Kamlet and R. Taft, *J. Am. Chem. Soc.*, 1976, **98**, 377–383.
26 C. Reichardt, *Pure Appl. Chem.*, 2004, **76**, 1903–1919.
27 T. V. Doherty, M. Mora-Pale, S. E. Foley, R. J. Linhardt and J. S. Dordick, *Green Chem.*, 2010, **12**, 1967–1975.
28 M. Ab Rani, A. Brant, L. Crowhurst, A. Dolan, M. Lui, N. Hassan, J. Hallett, P. Hunt, H. Niedermeyer and J. Perez-Arlandis, *Phys. Chem. Chem. Phys.*, 2011, **13**, 16831–16840.
29 Y. Fukaya, K. Hayashi, M. Wada and H. Ohno, *Green Chem.*, 2008, **10**, 44–46.
30 H. Ohno and Y. Fukaya, *Chem. Lett.*, 2009, **38**, 2–7.
31 A. Xu, J. Wang and H. Wang, *Green Chem.*, 2010, **12**, 268–275.
32 L. K. J. Hauru, M. Hummel, A. W. T. King, I. A. Kilpeläinen and H. Sixta, *Biomacromolecules*, 2012, **13**, 2896–2905.
33 J. Kahlen and K. Leonhard, *Green Chem.*, 2010, **12**, 2172–2181.
34 M. G. S. Chua and M. Wayman, *Can. J. Chem.-Rev. Can. Chim.*, 1979, **57**, 1141–1149.
35 J. B. Li, G. Henriksson and G. Gellerstedt, *Bioresour. Technol.*, 2007, **98**, 3061–3068.
36 H. L. Trajano, N. L. Engle, M. Foston, A. J. Ragauskas, T. J. Tschaplinski and C. E. Wyman, *Biotechnol. Biofuels*, 2013, 6.
37 N. Sathitsuksanoh, K. M. Holtman, D. J. Yelle, T. Morgan, V. Stavila, J. Pelton, H. Blanch, B. A. Simmons and A. George, *Green Chem.*, 2014, **16**, 1236–1247.
38 J. L. Wen, T. Q. Yuan, S. L. Sun, F. Xu and R. C. Sun, *Green Chem.*, 2014, **16**, 181–190.
39 A. George, K. Tran, T. J. Morgan, P. I. Benke, C. Berrueco, E. Lorente, B. C. Wu, J. D. Keasling, B. A. Simmons and B. M. Holmes, *Green Chem.*, 2011, **13**, 3375–3385.
40 R. H. Newman and J. A. Hemmingson, *Cellulose*, 1995, **2**, 95–110.
41 S. Park, D. K. Johnson, C. I. Ishizawa, P. A. Parilla and M. F. Davis, *Cellulose*, 2009, **16**, 641–647.
42 S. Park, J. O. Baker, M. E. Himmel, P. A. Parilla and D. K. Johnson, *Biotechnol. Biofuels*, 2010, 3.
43 N. Sathitsuksanoh, Z. G. Zhu, S. Wi and Y. H. P. Zhang, *Biotechnol. Bioeng.*, 2011, **108**, 521–529.
44 R. Arora, C. Manisseri, C. L. Li, M. D. Ong, H. V. Scheller, K. Vogel, B. A. Simmons and S. Singh, *Bioenergy Res.*, 2010, **3**, 134–145.
45 D. B. Fu and G. Mazza, *Bioresour. Technol.*, 2011, **102**, 7008–7011.
46 R. Kumar, G. Mago, V. Balan and C. E. Wyman, *Bioresour. Technol.*, 2009, **100**, 3948–3962.
47 R. C. Remsing, R. P. Swatloski, R. D. Rogers and G. Moyna, *Chem. Commun.*, 2006, 1271–1273.
48 J. B. Taylor, *Trans. Faraday Soc.*, 1957, **53**, 1198–1203.
49 A. E. Bennett, C. M. Rienstra, M. Auger, K. V. Lakshmi and R. G. Griffin, *J. Chem. Phys.*, 1995, **103**, 6951–6958.
50 M. Selig, N. Weiss and Y. Ji, Technical Report, NREL/TP-510-42629, National Renewable Energy Laboratory, Golden, CO, 2008.
51 A. Sluiter, B. Hames, R. Ruiz, J. Sluiter, D. Templeton and D. Crocker, Technical Report, NREL/TP-510-42618, National Renewable Energy Laboratory, Golden, CO, 2008.
52 A. Guerra, I. Filpponen, L. A. Lucia and D. S. Argyropoulos, *J. Agric. Food Chem.*, 2006, **54**, 9696–9705.
53 H. J. C. Berendsen, D. Vanderspoel and R. Vandrunen, *Comput. Phys. Commun.*, 1995, **91**, 43–56.
54 B. Hess, C. Kutzner, D. van der Spoel and E. Lindahl, *J. Chem. Theor. Comput.*, 2008, **4**, 435–447.
55 R. J. Woods, R. A. Dwek, C. J. Edge and B. Fraserreid, *J. Phys. Chem.*, 1995, **99**, 3832–3846.
56 J. M. Wang, R. M. Wolf, J. W. Caldwell, P. A. Kollman and D. A. Case, *J. Comput. Chem.*, 2004, **25**, 1157–1174.
57 W. L. Jorgensen, J. Chandrasekhar, J. D. Madura, R. W. Impey and M. L. Klein, *J. Chem. Phys.*, 1983, **79**, 926–935.
58 T. Darden, D. York and L. Pedersen, *J. Chem. Phys.*, 1993, **98**, 10089–10092.
59 B. Hess, H. Bekker, H. J. C. Berendsen and J. G. E. M. Fraaije, *J. Comput. Chem.*, 1997, **18**, 1463–1472.
60 S. Nose and M. L. Klein, *Mol. Phys.*, 1983, **50**, 1055–1076.

